Quantitative Analyses of Morphological Data

Philippe Blondel

Abstract Submarine morphologies are complex and analysed based on shapes, dimensions and internal variations. They are also analysed based on their surroundings. This chapter starts by comparing the sensors providing this information: most of them are based on remote sensing (acoustic/electromagnetic). They produce Digital Terrain Models (DTMs), corresponding to regularly sampled (and/or interpolated) grids. Illustrated with regular examples, the chapter shows the basic measurements used to describe and compare morphologic data, their variations with multi-scale approaches (e.g. Fourier space, fractals) and how this can be used to identify trends and patterns. Geographic Information Systems and the emerging applications of Artificial Intelligence and data mining are also presented.

1 Mapping Submarine Morphologies

Geological structures on the seabed or below are analysed based on their shapes, their dimensions and their internal variations. They are also compared to their general surroundings, to provide more context and refine their interpretation. For example, sand ripples are recognised as elongate structures with relatively small heights, occurring in groups of generally similar characteristics and situated in shallow waters susceptible to wave action. Variations in their directions, their relative dimensions and their sedimentary composition might provide additional information on their emplacement and evolution with time. Volcanic edifices will generally present circular or sub-circular shapes, with clear variations in topography associated with dome emplacement and additional cones; individual lava flows will give information about eruption stages, their types and their relative chronologies. But where does this morphologic information come from?

The previous chapters have presented a variety of techniques, most of them based on remote sensing: sidescan sonar (Chapter "Sidescan Sonar"), multibeam

P. Blondel (✉)
Department of Physics, University of Bath, Bath, UK
e-mail: P.Blondel@bath.ac.uk

A. Micallef et al. (eds.), *Submarine Geomorphology*, Springer Geology,
DOI 10.1007/978-3-319-57852-1_5

echo sounder (Chapter "Multibeam Echosounders"), and seismics (Chapter "Reflection and Refraction Seismic Methods"). The following chapters will present direct physical sampling (Chapter "Seafloor Sediment and Rock Sampling") and localised surveys with bespoke subsea platforms (Chapter "ROVs and AUVs"), although the former might not always measure morphology directly. Other approaches worthy of mention are the emerging uses of airborne lidar (e.g. Vrbancich, in Blondel 2012), airborne or spaceborne synthetic-aperture radar (e.g. Marghany, also in Blondel 2012), and subsea stereo-photogrammetry (Pouliquen et al. 2002, see also Chapter "ROVs and AUVs"). This multiplicity of tools is highlighted by Lecours et al. (2016), who review the different applications and advocate combining sensors and data sources as much as possible [the related discussion paper by Mitchell (2016) offers helpful comments too].

This chapter will assume a reasonably accurate Digital Terrain Model (DTM) has been created, with a final resolution commensurate with the processes of interest. This DTM will most likely have been created by acoustic remote sensing. Because of their large swath coverage and increasing resolutions, multibeam echosounders are often and rightly considered the tools of choice to measure morphology (as shown in Chapter "Multibeam Echosounders"). Ideally, their measurements have been processed to international standards, e.g. the International Hydrographic Organisation (IHO) standards S-44 for hydrographic surveys (https://www.iho.int/iho_pubs/standard/S-44_5E.pdf). Primarily intended for navigation, their accuracy means this standard is still fully relevant to geomorphologists. De facto standards are also recommended for processing multibeam backscatter (Lurton and Lamarche 2015, and references therein), as it provides other information about topography. To a lesser extent, sidescan sonars can provide comparable information, either by design (interferometric sonars), by operation (multi-angle operation) or through additional processing (for example deriving heights and shapes of protruding objects imaged at grazing angles, although this is strongly limited by the grazing angles used, see also Chapter "Sidescan Sonar").

The interactions of acoustic waves with the seabed are complex and presented in multiple textbooks (e.g. Blondel 2009; Lurton 2010). The first contributor to acoustic reflectivity is the slope of the surface being imaged (Fig. 1a). Because of the size of the sonar footprint at this location, the actual depth will vary between the centre of the footprint (average) and its edges (minimum and maximum values). Depending on how acoustic returns are processed, the depth returned to the user might be any value within the full range (ideally the median or the mean). The acoustic reflectivity will be also extremely sensitive to the micro-scale roughness of the seabed, at scales comparable to the imaging wavelength (for a 150 kHz sonar, this would be roughly 1 cm). Because of the wavelengths used to quantify seabed morphologies, this is generally less of an issue. The third and smallest contributor to acoustic reflectivity will in fact become the second largest contributor to depth accuracies: depending on seabed type and imaging frequencies, the sonar waves might travel within the immediate sub-seabed, and acoustic returns might come from deeper than expected. This is seen with dual-frequency systems: Blondel and Pouliquen (2004) show for example how 100-kHz maps show returns from the top

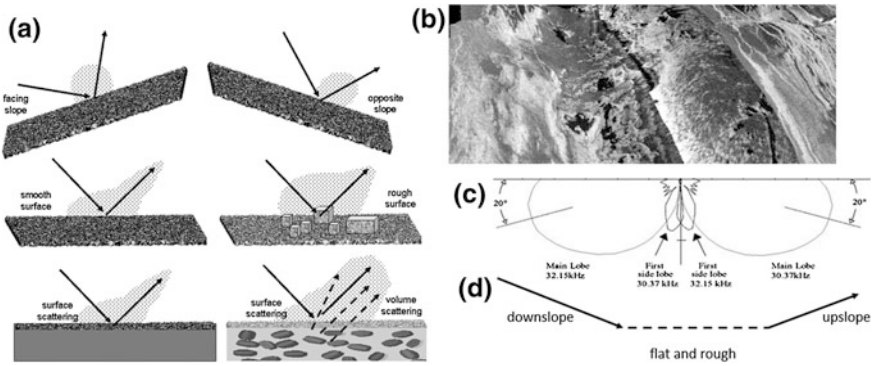

Fig. 1 **a** The scattering of waves (acoustic or electromagnetic) from a complex surface will be affected by its orientation, how rough it is (relative to the imaging wavelength) and how deep below the surface waves can penetrate and scatter; **b** this typical image of a mid-ocean ridge combines sidescan sonar imagery and multibeam bathymetry; **c** its interpretation needs to take into account the beam pattern of the imaging sonar(s); **d** the slopes facing toward or away from the sonar also need to be considered. Figure modified after Blondel (2009)

of underwater vegetation, whereas simultaneous 384-kHz measurements show slightly deeper returns from the seabed itself. In extreme cases, e.g. with low-frequency sonars such as GLORIA (6.5 kHz), it is possible to detect structures well below a thick mud cover (Moore et al. 1989). Care should therefore always be taken when using sonar measurements, and it is necessary to check whether the acoustic waves can actually show returns from deeper in the seabed than expected.

2 Quantitative Structures, Shapes and Their Variations

Seabed morphology is inherently complex, both at regional and local scales. Figure 2 shows idealised landforms in a sedimentary environment. Other landforms not represented here would include volcanic constructs (from lava flows to small cones or large domes), large faults and landslides (potentially with different debris slides), hydrothermal areas (with small and large edifices, deposits and small fissures), and any seabed affected by marine life (e.g. vegetation, burrowing) or human activities (from shipwrecks to cables or caissons). Readers interested in how these other structures look like when imaged with sonars are invited to read the "Handbook of Sidescan Sonar" (Blondel 2009), which provides many examples from around the world. The key points here are how these different generic shapes can be detected, quantified and analysed.

At a regional scale, the seabed is best characterised by its regular sloping topography, best revealed by comparison of along-slope profiles. Local variations are visible, for example, the canyon in the middle of the sketch (Fig. 2). Two-dimensional

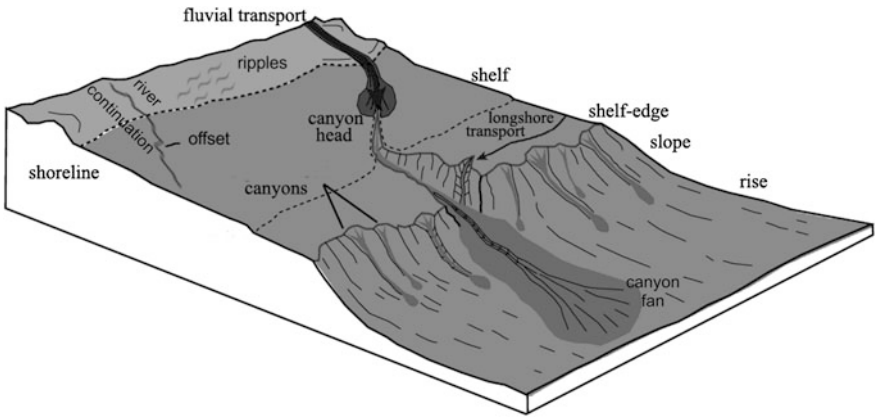

Fig. 2 Typical sedimentary shore, showing a variety of morphologic structures. Baseline figure from Obelcz et al. (2014) with permission from Elsevier

analyses of the shelf edges and slopes would reveal more about the dynamic sedimentary regimes, in particular along-shore transport of sediments. Finer-scale analyses (in 2-D) would reveal the presence of sand ripples in the shallow waters exposed to wave action, and 3-D analyses might show differences in their formation and evolution. Small structures like underwater prolongation of rivers (top left) might also show offsets, indicative of tectonic activity. Larger structures, like the canyon fan (bottom right) would need quantifying in 2-D and 3-D to show variations in sediment supplies and links to the geology (and morphology) of deeper waters.

Practically speaking, this means the geomorphologist needs to analyse 2-D profiles and 3-D sections of parts of the DTM. In the case of a submarine canyon (Fig. 3, left), cross-sections taken at regular intervals can reveal canyon evolution and depth variations, steep slopes and potential asymmetry, and variations in sediment deposits in the canyon and on its banks. Repeat surveys can be used to measure steepening of the slopes, or further changes, which might lead to geo-hazards. Figure 3 (top right) shows a portion of the Mid-Atlantic Ridge, with high-resolution data near the ridge axis and lower-resolution bathymetry away from the active part of the ridge. Cross-sections (Fig. 3, bottom right) will reveal different processes depending on the scale at which these measurements are made, highlighting the need for high resolution. Lecours et al. (2016) recommend "extending the analysis beyond the basic 3 × 3 neighbourhood […] as it facilitates the identification of spatial scales" relevant to specific processes. This multi-scale analysis should be a necessity, and not just a recommendation, as it is the only way to enable meaningful comparisons between datasets measured with different sensors.

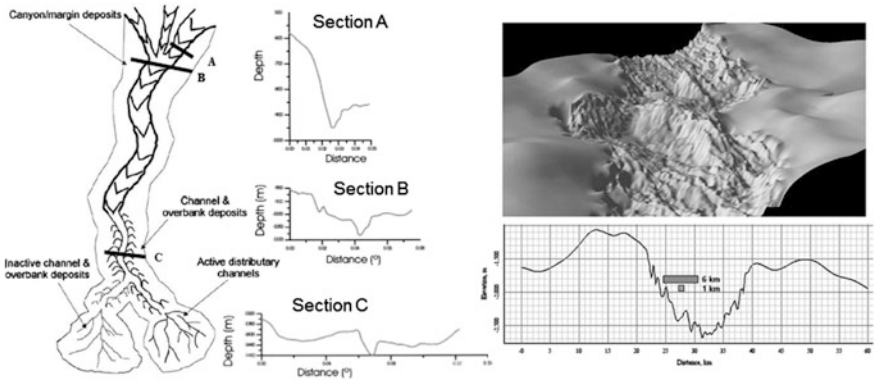

Fig. 3 *Left* successive analyses of bathymetric profiles across a submarine canyon reveal its evolution, with steep, unconsolidated slopes (*Section A*) and several levels of deposits (*Sections B and C*). Modified after Gómez Sichi et al. (2005). *Right* Bathymetry from the Mid-Atlantic Ridge (from the R2K database) is compiled with high resolution near the ridge axis and lower resolution data away from the main segments (*top*). Bathymetric profiles will reveal different information based on their resolution (*bottom*). Modified after Blondel (2009)

3 Geostatistics to Geographical Information Systems

3.1 Basic Measurements

A bathymetric profile across a surface of interest can be expressed as a collection of points, with depths *z(i)*, measured at *N* points regularly spaced (and denoted with index *i*, varying from 1 to *N*). The first parameter of interest will be the average depth $\langle z \rangle$:

$$\langle z \rangle = \frac{1}{N} \sum_{i=1}^{N} z(i) \tag{1}$$

If choosing a reference depth z_0, the average height <*h*> will be calculated with reference to the relative depths $z(i) - z_0$, giving rise to a similar equation:

$$\langle h \rangle = \frac{1}{N} \sum_{i=1}^{N} (z(i) - z_0) \tag{2}$$

For a portion of the map, assumed square for simplicity (i.e. *N* points along one direction and *N* points along the orthogonal direction), the average depth is then expressed as:

$$\langle z \rangle = \frac{1}{N^2} \sum_{i=1}^{N} \sum_{j=1}^{N} z_{i,j} \tag{3}$$

The next equations will follow the same assumption of a square sampling, justified if the original measurements have been processed with square gridding (which is the case in most software now) or interpolated to the same resolution along both axes. Changing to non-square samples is mathematically straightforward, replacing N with M where needed. All subsequent equations can also be adapted simply to profiles along a single direction (using only one summation, for example).

The average height or depth does not account for small-scale variations, which can be very important in describing the surface (e.g. for talus deposits or for lava flows). From an acoustic point of view, the roughness will also be indicative of the likely scattering processes (cf. Blondel 2009). The average roughness, also called rms roughness, is traditionally calculated as:

$$z_0 = \sqrt{\frac{1}{N^2 - 1} \sum_{i=1}^{N} \sum_{j=1}^{N} \left(z_{i,j} - \langle z \rangle \right)^2} \tag{4}$$

This roughness can be biased if the underlying surface is on a slope, and it is often recommended to measure the rms tilt over a range Δx:

$$s_0 = \frac{\sqrt{\left\langle \left(z(x) - z(x + \Delta x) \right)^2 \right\rangle}}{\Delta x} \tag{5}$$

This tilt can be used to remove the underlying surface from the measurements, if it is regular enough or known well enough. This operation is often known as de-trending, and it requires accurate assessment of what the background surface is like, or should be like, to avoid biasing the final results.

Local slopes are also of interest, as they can be used to delineate features. The slope gradient is defined as the maximum rate of elevation change, and it can be calculated over different ranges (in some datasets, using the maximum resolution available can indeed add noise and it is then necessary to apply simple low-pass filters, for example 3×3 moving averages). In its simplest form, the slope gradient is defined as:

$$gradient = atan\left(\left(\frac{\partial z}{\partial x} \right)^2 + \left(\frac{\partial z}{\partial y} \right)^2 \right) \tag{6}$$

Variations in slope gradients over large areas can be used to distinguish terrains based on their statistical differences, and not on any qualitative interpretations.

Micallef et al. (2012) use, for example, the cumulative frequency distribution of slope gradients to identify points of inflection. This allows the quantitative separation of morphological units such as flat zones, sloping zones, crests, depressions and breaks of slopes. Shaw and Smith (1990) quantify the spatial correlation of these variations with auto-covariance functions to distinguish very different types of heterogeneous terrains.

A tool now frequently used by marine geomorphologists (e.g. Verfaillie et al. 2007) is the Bathymetry Position Index (BPI). Implemented in common software like ArcGIS™, the BPI algorithm measures height differences between a focal point and the average calculated over surrounding cells within a user-defined shape (which can therefore be square, but can also be restricted to a specific morphological feature like a canyon or depression). By definition, negative BPIs correspond to local depressions and positive BPIs to crests.

The BPI can be used in conjunction with the topographic ruggedness index (TRI), introduced by Riley et al. (1999). The TRI measures the square root of the average of squared height differences between a centre point and the closest measurements (i.e. 8 measurements for a square grid).

More complex equations can quantify other parameters of interest, like the profile curvature, which represents the maximum change in slope gradients between adjacent cells in a chosen neighbourhood. It is used for example to identify convex and concave breaks of slope (i.e. faults, fissures and steep escarpments). It is defined by Micallef et al. (2012) by looking at derivatives of the height z over orthogonal directions x and y (over at least 3 consecutive points, but any range can be considered):

$$Curvature = -\frac{\left(\frac{\partial z}{\partial x}\right)^2 \times \frac{\partial^2 z}{\partial x^2} + 2 \times \frac{\partial z}{\partial x} \times \frac{\partial z}{\partial y} \times \frac{\partial^2 z}{\partial x \partial y} + \left(\frac{\partial z}{\partial y}\right)^2 \frac{\partial^2 z}{\partial y^2}}{\left(\left(\frac{\partial z}{\partial x}\right)^2 + \left(\frac{\partial z}{\partial y}\right)^2\right)\left(1 + \left(\frac{\partial z}{\partial x}\right)^2 + \left(\frac{\partial z}{\partial y}\right)^2\right)^{\frac{3}{2}}} \tag{7}$$

Once identified on the maps, for example through image processing or geostatistics, some morpho-geological units can be quantified with other parameters, like their lengths, widths, areas or volumes (if knowing where the base of the unit is likely to be). For submarine canyons and other similar features, it is often interesting to calculate the sinuosity index *SI*, defined as the ratio of the length along the structure to the straight distance between its extremities (Euclidean distance). In terrestrial geomorphology (e.g. Mueller 1968), these values are traditionally interpreted as "almost straight" ($SI < 1.05$), "winding" ($1.05 \leq SI < 1.25$), "twisty" ($1.25 \leq SI < 1.50$) and "meandering" ($SI > 1.50$). For closed structures, other parameters of interest will be the overall shape, which can be characterised with tools like the Hough transform or by measures of similarity with expected shapes (circles, ellipses, etc.). More information can be derived from combining different measurements (e.g. principal axes of several structures, lengths, widths, slope histograms), as shown in Shaw and Smith (1987), inter alia.

3.2 Variations with Spatial Scales

If regular enough, i.e. occurring at specific spatial internals (or wavelengths), morphogeological variations show a range of spatial frequencies (not to be confused with the imaging frequency). This is best measured using simple Fourier transforms, whose values are calculated at different spatial frequencies *f*:

$$F(f) = \int_{-\infty}^{+\infty} z(x) e^{-i\,2\pi f\,x} dx \tag{8}$$

From a mathematical point of view, the integral sign is used to denote summation over samples as close as possible to each other, and over as large a range as possible ($-\infty$ and $+\infty$). In practice, the use of finite ranges of integration will limit the frequencies measurable.

Power spectral densities *W(f)* are a good way to check which frequencies are predominant:

$$W(f) = \frac{1}{L}\left(\mathrm{Re}(F(f))^2 + \mathrm{Im}(F(f))^2\right) \tag{9}$$

For example, sand ripples with a spacing *X* will have much higher power in the spatial frequency 1/*X*. Ripple systems with different heights, different widths and different distances will show in the Fourier spectra with different spatial frequencies (along each direction chosen), and this might be used to highlight overlain ripple fields, or assess how they degrade with currents or wave action. Other types of decompositions, e.g. with wavelet transforms, are available; they will not be presented here, but their use should always keep in mind how much physical reality can be represented with specific mathematical functions.

The role of scale is important, as it is conditioned by the data acquisition (resolution of the mapping sensor and small-scale accuracy), by the processing (quality of the interpolation and gridding schemes used) and by the physical processes themselves. The Nyquist theorem states that measurements should cover at least twice the frequency to analyse. A topographic process changing every 2 m would need measuring at least every 1 m to get an accurate representation of its variability. And the number of measurements is commensurate with the parameter to derive. For example, if using a bathymetry dataset with 10-m resolution, calculating the local slope uses 3 points, i.e. distances of 30 m. Mean slopes need to average over 3 values or more, i.e. distances close to 100 m (calculating local slopes every 10 m would bias the measurements, as neighbouring points will include similar bathymetry values).

Sometimes, measurements made over particular spatial scales will be very different if done over different scales. This was first formalised by Mandelbrot (1967), who described how the size of complex lengths/surfaces will increase as the

measuring unit decreases. This can be plotted as a logarithmic function, indicative of the fractal dimension D (in this case, the slope of the function equates $D - 1$). This started the research into fractals, also known as self-affine or fractional Brownian statistics (more detailed information is available at: http://www.math.yale.edu/mandelbrot/).

Variations of heights with the horizontal measurement scale L follow power laws and can for example be used to derive a scaling constant C_H and a quantity H (known as the Hurst exponent and in the range 0–1):

$$\langle h \rangle = C_H \times \left(\frac{L}{L_0} \right)^H \tag{10}$$

C_H is the rms height when $L = L_0$, and the fractal dimension is directly related to the Hurst exponent:

$$\begin{cases} D = 2 - H & (for\ a\ profile) \\ D = 3 - H & (for\ a\ surface) \end{cases} \tag{11}$$

In the case of radar remote sensing of planetary surfaces, these parameters can be used to easily distinguish between lava flows, such as smooth pahoehoe ($H = 0.63$, $C_H = 0.05$), rough pahoehoe ($H = 0.48$ and $C_H = 0.16$) and a′a ($H = 0.26$, $C_H = 0.24$) (Campbell 2011). Fractal dimensions can therefore be considered a measure of roughness, at least in this case.

Fractals are very useful to describe scale-independent processes, i.e. processes which will produce the same results at small and large scales. In some cases, the processes are more complex and cannot be described with a single fractal dimension consistent at all scales (multifractals) (e.g. Ijjasz-Vasquez et al. 1992). The mathematics can rapidly become complex and thus will not be treated here. Interested readers can find more in books and articles by Benoit Mandelbrot, who founded this field, and look at applications to seabed morphologies in Mareschal (1989), Malinverno (1989) and Goff et al. (1993).

3.3 Finding Trends and Patterns

There are many other measures than those presented in the previous two sub-sections. All should be related to physically meaningful descriptions of the seabed and of morphological structures. Some metrics, e.g. lengths, widths, directions, can be directly associated to geological processes, for example the evolution of a submarine canyon. Other metrics might be more difficult to interpret, and this is where data can be usefully compared to expected distributions.

Simple bathymetric profiles, for example, can be interpreted as the combination of a background profile, associated to the regional slope, systematic deviations, associated to local processes, and random or pseudo-random smaller deviations.

Auto-regressive (AR) models and auto-regressive moving-average (ARMA) derivations can be used to unravel the local and regional contributions (see Box et al. 2015 for examples in a variety of domains). More deterministic approaches have been followed, for example matching existing profiles to spline functions and relating each base function to a specific geological process.

Surface analyses have similarly aimed at separating the stochastic part of the seafloor morphology from more local (and/or random) processes. Goff and Jordan (1989) used the covariance of bathymetry to study abyssal hill formation in different regions, taking great care to remove the effects of data acquisition and resolution. Mitchell (1996) designed a technique to automatically fit paraboloid shapes to bathymetry, and used this approach to interpret transport processes at continental slopes (Mitchell and Huthnance 2007). The field of pattern-matching is vast, and these are only two examples, selected because they are perfect demonstrations of how to match theoretical patterns to existing data, within the constraints of how it was acquired, and how to derive meaningful interpretations of geomorphological processes.

Geographic Information Systems (GIS) combine datasets and measurements in geo-located and inter-comparable databases. They allow direct query of specific characteristics (e.g. "can sediment flow from this canyon affect this area downslope?", "how far are hydrothermal vents from small-scale fissures?"). Many examples are currently available on the market, and to cite but one, ArcGIS™ seems rather prevalent at the moment, with new tools specifically built for the geomorphological community (e.g. Rigol-Sanchez et al. 2015; Kelner et al. 2016). Other techniques, such as multivariate analyses (e.g. Husson et al. 2009), neural networks (e.g. Mallat 2016), or Artificial Intelligence (e.g. Gvishiani and Dubois 2002) aim to extend this guided approach by exploring how subsets of the data might relate to each other. Used in many other data-rich fields, the new discipline of data mining is likely to revolutionise submarine morphometry (e.g. Wan et al. 2010; Planella Gonzalez et al. 2013). One *caveat* is that market leaders, and any GIS for that matter, should always clearly present the rationale behind the calculations, avoiding a "black box" approach where numbers lose their meaning by not being testable or not matching a physical meaning. This is often why some communities rely on programming languages like Matlab or R (e.g. Husson et al. 2009) to keep this important open-source aspect.

4 Conclusions

Modern sensors can map the seabed at spatial resolutions varying from a kilometre (for the oldest generation) to sub-metre (for most systems available now), with depth accuracies generally below a metre. The resulting datasets are extremely large and they can provide important information on the morphology of the seabed, on the formation and evolution of different structures, and how they are affected with time (for example when doing repeat surveys). It is therefore important to quantify

accurately the different morphologies and to be able to relate them to geologically meaningful processes.

This chapter introduced some of the key metrics for morphology, selected on the basis of simplicity and demonstrated applicability to remote sensing (acoustic or electromagnetic). From simple profiles to surfaces and volumes, these measurements aim at quantifying the underlying processes. How accurate they are depends on how good the measurements are, and how well their potential limitations are understood (imaging accuracy, combination of different resolutions, role of volume scattering vs. surface scattering). The use of multiple resolutions is highlighted as it can provide important information when geological processes are superposed in space. The development of Geographic Information Systems offers very useful tools to the interpreters, provided the mathematical details of the different metrics are well understood, traceable and comparable. Applications of data mining and Artificial Intelligence to submarine morphology are appearing and also proving very attractive.

References

Blondel P (ed) (2012) Bathymetry and its applications. In Tech. Open Access: http://www.intechopen.com/books/show/title/bathymetry-and-its-applications. doi:10.5772/2132

Blondel P, Pouliquen E (2004) Acoustic textures and detection of shipwreck cargo—example of a Roman ship near Elba, Italy. In: Akal T, Ballard RD, Bass GD (eds) Proceedings of first internal congress on the application of recent advances in underwater detection and survey techniques to underwater archaeology, pp 135–142

Blondel P (2009) Handbook of sidescan sonar. Springer, Berlin

Box G, Jenkins GM, Reinsel GC (2015) Time series analysis: forecasting and control, 4th edn. Prentice-Hall, Englewood Cliffs

Campbell BA (2011) Radar remote sensing of planetary surfaces. Cambridge University Press, Cambridge

François H, Lê S, Pagès J (2009) Exploratory multivariate analysis by example using R. CRC-Press, London

Goff JA, Jordan TH (1989) Stochastic modelling of seafloor morphology: resolution of topographic parameters by sea beam data. IEEE J Oceanic Eng 14(4):326–337

Goff JA, Malinverno A, Fornari DJ, Cochran JR (1993) Abyssal hill segmentation: quantitative analysis of the East Pacfic rise flanks 7°S–9°S. J Geophys Res 98(B8):13851–13862

Gómez Sichi O, Blondel Ph, Grácia E, Dañobeitia JJ (2005) Quantitative textural analyses of TOBI sonar imagery along the Almería Canyon (Almería Margin, Alborán Sea, SE Spain). In: Hodgson DM, Flint SS (eds) Submarine slope systems: processes and products, vol 244. Geological Society Special Publication, London, pp 141–154

Gvishiani A, Dubois JO (2002) Artificial intelligence and dynamic systems for geophysical applications. Springer, Berlin

Ijjasz-Vasquez EJ, Rodriguez-Iturbe I, Bras RL (1992) On the multifractal characterization of river basins. Geomorphology 5(3):297–310

Kelner M, Migeon S, Tric E, Couboulex F, Dano A, Lebourg T, Taboada A (2016) Frequency and triggering of small-scale submarine landslides on decadal timescales: analysis of 4D bathymetric data from the continental slope offshore Nice (France). Mar Geol 379:281–297

Lecours V, Dolan MFJ, Micallef A, Lucieer VL (2016) A review of marine geomorphometry, the quantitative study of the seafloor. Hydrol Earth Syst Sci 20:3207–3244

Lurton X (2010) An introduction to underwater acoustics—principles and applications. Springer, Heidelberg

Lurton X, Lamarche G (eds) (2015) Backscatter measurements by seafloor-mapping sonars. Guidelines and recommendations. http://geohab.org/wp-content/uploads/2014/05/BSWG-REPORT-MAY2015.pdf. Accessed 24 Oct 2016

Malinverno A (1989) Segmentation of topographic profiles of the seafloor based on a self-affine model. IEEE J Oceanic Eng 14(4):348–359

Mallat S (2016) Understanding deep convolutional networks. Phil Trans R Soc A 374:20150203. doi:10.1098/rsta.2015.0203

Mandelbrot BB (1967) How long is the coast of Britain? Stat self-similarity and fractional dimension. Science 156(3775):636

Mareschal J-C (1989) Fractal reconstruction of sea-floor topography. Pure Appl Geophys 151:197–210

Micallef A, Le Bas TP, Huvenne VA, Blondel P, Hühnerbach V, Deidun A (2012) A multi-method approach for benthic habitat mapping of shallow coastal areas with high-resolution multibeam data. Cont Shelf Res 39–40:14–26

Mitchell NC (1996) Processing and analysis of Simrad multibeam sonar data. Mar Geophys Res 18:729–739

Mitchell N (2016) Interactive comment on "Characterising the ocean frontier: a review of marine and coastal geomorphometry" by Lecours V et al. Hydrol Earth Syst Sci Discuss. doi:10.5194/hess-2016-73-RC1

Mitchell NC, Huthnance JM (2007) Comparing the smooth, parabolic shapes of interfluves in continental slopes to predictions of diffusion transport models. Mar Geol 236:189–208

Mueller J (1968) An introduction to the hydraulic and topographic sinuosity indexes (1). Ann Assoc Am Geogr 58(2):371–385

Moore JG, Clague DA, Holcomb RT, Lipman PW, Normark WR, Torresan ME (1989) Prodigious submarine landslides on the Hawaiian Ridge. J Geophys Res 94(B12):17465–17484

Obelcz J, Brothers D, Chaytor J, ten Brink U, Ross SW, Brooke S (2014) Geomorphic characterization of four shelf-sourced submarine canyons along the U.S. Mid-Atlantic continental margin. Deep Sea Res II 104:106–119

Planella Gonzalez LF, Gomez Pivel MA, Alcoba Ruiz DD (2013) Improving bathymetric images exploration: a data mining approach. Comput Geosci 54:142–147

Pouliquen E, Blondel P, Canepa G, Hollett R (2002) Multi-sensor analysis of the seabed in shallow-water areas: overview of the MAPLE-2001 experiment. In: Proceedings of sixth European conference on underwater acoustics ECUA-2002, Gdansk, Poland, pp 167–175

Rigol-Sanchez JP, Stuart N, Pulido-Bosch A (2015) ArcGeomorphometry: a toolbox for geomorphometric characterisation of DEMs in the ArcGIS environment. Comput Geosci 85:155–163

Riley SJ, DeGloria SD, Elliot R (1999) A terrain ruggedness index that quantifies topographic heterogeneity. Intermt J Sci 5(1–4):23–27

Shaw PR, Smith DK (1990) Robust description of statistically heterogeneous seafloor topography through its slope distribution. J Geophys Res 95(B6):8705–8722

Shaw PR, Smith DK (1987) Statistical methods for describing seafloor topography. Geophys Res Lett 14:1061–1064

Verfaillie E, Doornenbal P, Mitchell AJ, White J, Van Lancker V (2007) The bathymetric position index (BPI) as a support tool for habitat mapping. Worked example for the MESH Final Guidance, 14 pp. (http://www.emodnet-seabedhabitats.eu/PDF/GMHM4_Bathymetric_position_index_(BPI).pdf). Last accessed 06 Feb 2017

Wan S, Lei TC, Chou TY (2010) A novel data mining technique of analysis and classification for landslide problem. Nat Hazards 52:211. doi:10.1007/s11069-009-9366-3